



# Effect of gas-liquid flow pattern and microbial diversity analysis of a pilot-scale biotrickling filter for anoxic biogas desulfurization



Fernando Almenglo<sup>a</sup>, Tercia Bezerra<sup>b</sup>, Javier Lafuente<sup>b</sup>, David Gabriel<sup>b</sup>,  
Martín Ramírez<sup>a,\*</sup>, Domingo Cantero<sup>a</sup>

<sup>a</sup> Department of Chemical Engineering and Food Technologies, Faculty of Sciences, University of Cadiz, Campus de Excelencia Agroalimentario ceiA3, 11510, Puerto Real, Cádiz, Spain

<sup>b</sup> GENOCOV Research Group, Department of Chemical, Biological and Environmental Engineering, School of Engineering, Universitat Autònoma de Barcelona, 08193, Bellaterra, Barcelona, Spain

## HIGHLIGHTS

- Alternative operation between co- and counter-current enhance the carrier lifetime.
- Elemental Sulfur cleaning can be carried out stopping the biogas feeding.
- *Sedimenticola* was consider the main desulfurizing bacteria.
- Single-pass reduce the H<sub>2</sub>S elimination capacity.

## ARTICLE INFO

### Article history:

Received 7 February 2016

Received in revised form

5 May 2016

Accepted 8 May 2016

Available online 24 May 2016

Handling Editor: Y Liu

### Keywords:

Biotrickling filter

Anoxic

Biogas desulfurization

Hydrogen sulfide

Pyrosequencing

## ABSTRACT

Hydrogen sulfide removal from biogas was studied under anoxic conditions in a pilot-scale biotrickling filter operated under counter- and co-current gas-liquid flow patterns. The best performance was found under counter-current conditions (maximum elimination capacity of 140 gS m<sup>-3</sup> h<sup>-1</sup>). Nevertheless, switching conditions between co- and counter-current flow lead to a favorable redistribution of biomass and elemental sulfur along the bed height. Moreover, elemental sulfur was oxidized to sulfate when the feeding biogas was disconnected and the supply of nitrate (electron acceptor) was maintained. Removal of elemental sulfur was important to prevent clogging in the packed bed and, thereby, to increase the lifespan of the packed bed between maintenance episodes. The larger elemental sulfur removal rate during shutdowns was 59.1 gS m<sup>-3</sup> h<sup>-1</sup>. Tag-encoded FLX amplicon pyrosequencing was used to study the diversity of bacteria under co-current flow pattern with liquid recirculation and counter-current mode with a single-pass flow of the liquid phase. The main desulfurizing bacteria were *Sedimenticola* while significant role of heterotrophic, opportunistic species was envisaged. Remarkable differences between communities were found when a single-pass flow of industrial water was fed to the biotrickling filter.

© 2016 Elsevier Ltd. All rights reserved.

## 1. Introduction

Sulfide oxidation coupled to denitrification by sulfide-oxidizing nitrate-reducing bacteria (SO-NR) in anoxic biotrickling filters (BTFs) has been shown as an alternative for biogas desulfurization. Overall, the process is similar to the aerobic process in terms of reactor design, packing material and operating conditions

(Almenglo et al., 2016; Montebello et al., 2014; Soreanu et al., 2008). The main difference lays in the use of nitrate as electron acceptor instead of oxygen. Nitrate use leads to no biogas dilution, thus no energy potential of biogas is lost, coupled to a reduced risk of explosion compared to that of oxygen.

Most BTFs for biogas desulfurization operate under a counter-current configuration (Muñoz et al., 2015). However, recently was found that oxygen mass transfer efficiency in the packed bed of an aerobic BTF filled with plastic Pall rings was more favorable in the case of a co-current configuration (López et al., 2016). The sulfate production capacity was 102.8 gS-H<sub>2</sub>S m<sup>-3</sup> h<sup>-1</sup> and 78.8 gS-H<sub>2</sub>S

\* Corresponding author.

E-mail address: [martin.ramirez@uca.es](mailto:martin.ramirez@uca.es) (M. Ramírez).

$\text{m}^{-3} \text{h}^{-1}$  for co-current and counter-current flow modes, respectively.

Despite the recent advances in the analysis of the impact of process variables on system performance both at laboratory and at pilot-scale, dynamics of microbial communities in anoxic biotrickling filters has been poorly referenced. There are many biological techniques to assess the microbial diversity as well as its evolution along time such as banding patterns from denaturing gradient gel electrophoresis (DGGE), fluorescence in-situ hybridization (FISH), terminal restriction fragment length polymorphism (T-RFLP) and pyrosequencing. However, pyrosequencing has been shown as one of the most powerful tools to analyze and quantify the microbial composition and abundance of biomass in bioreactors under different operating conditions (Cheng et al., 2016; Portune et al., 2014; Montebello et al., 2013). To the authors' knowledge, no microbial analysis based on pyrosequencing has been performed in anoxic BTFs.

In the present work, the effect of the co- and counter-current G-L flows and the effect of a single-pass of supplied industrial water were assessed on bioreactor performance as well as on the microbial diversity and its dynamics based on Tag-encoded FLX amplicon pyrosequencing (bTEFAP).

## 2. Materials and methods

### 2.1. Experimental equipment and analytical methods

An anoxic BTF at pilot-scale was used, which characteristics can be found elsewhere (Almenglo et al., 2016). The column diameter and packing bed height were 0.5 and 0.85 m, respectively. Randomly filled, open-pore polyurethane foam (PUF) cubes of  $125 \text{ cm}^3$  each were used as packing material. The BTF was installed at the 'Bahía Gaditana' (San Fernando, Spain) wastewater treatment plant (WWTP) and fed with a biogas split from one of their full-scale anaerobic digesters. Thus, temperature and pH were not controlled. Industrial water (IW) from the WWTP was used to feed the BTF. The IW was supplemented with a nitrate concentrate solution as described by Almenglo et al. (2016).

The biotrickling was operated for a period of 415 days in five well-differenced operational periods. The first 297 days the BTF was operated in counter-current mode, then the biogas was fed in co-current for 63 days (days 298–360). After that, the biogas supply was disconnected to allow the removal of elemental sulfur for 7 days (days 361–367) and returned to counter-current for 34 days (days 368–401) to reach steady-state conditions before the single-pass flow study for 14 days (days 402–415).

The  $\text{CH}_4$ ,  $\text{CO}_2$  and  $\text{H}_2\text{S}$  concentrations in the biogas stream were measured using a gas chromatograph (GC-450, BRUKER, Germany). A specific gas sensor (GA2000Plus, Fonotest Instruments S.L., Spain) was used for field measurements. Sulfate, nitrite and nitrate were measured by colorimetric methods (Almenglo et al., 2016; Clesceri et al., 1999). Sulfide was measured using an ion-selective electrode (ISE) for sulfide combined with an Ag/AgCl electrode as reference (sympHony™ Meter, VWR International Inc., USA). Dissolved oxygen (DO) was measured using a polarographic sensor (YSI MODEL 95, YSI incorporated, USA).

### 2.2. Mass transfer coefficient determination

The gas-liquid mass transfer coefficient was determined using pristine PUF and IW. Initially, a biogas stream was passed through the column to desorb DO. Then, an air stream was fed to the BTF while DO was recorded at the inlet and outlet of the packed bed ( $T = 22.6 \pm 0.8 \text{ }^\circ\text{C}$ ). The water phase was continuously recirculated from bottom to top of the BTF. Same considerations as these applied

by Dorado et al. (2009) were assumed in order to obtain equations (1)–(3).

$$Q_L(C_{L,out} - C_{L,in}) = K_L a V_C \frac{\left(\frac{C_{G,in}}{H} - C_{L,out}\right) - \left(\frac{C_{G,out}}{H} - C_{L,in}\right)}{\ln\left(\frac{\frac{C_{G,in}}{H} - C_{L,out}}{\frac{C_{G,out}}{H} - C_{L,in}}\right)} \quad (1)$$

$$f_1(C) = V_C \frac{\left(\frac{C_{G,in}}{H} - C_{L,out}\right) - \left(\frac{C_{G,out}}{H} - C_{L,in}\right)}{\ln\left(\frac{\frac{C_{G,in}}{H} - C_{L,out}}{\frac{C_{G,out}}{H} - C_{L,in}}\right)} \quad (2)$$

$$Q_L(C_{L,out} - C_{L,in}) = K_L a f_1(C) \quad (3)$$

Where  $Q_L$  is the liquid flow rate ( $\text{m}^3 \text{h}^{-1}$ );  $C_{L,out}$  and  $C_{L,in}$  are the outlet and inlet DO concentration ( $\text{g O}_2 \text{m}^{-3}$ ) of the packed bed, respectively;  $C_{G,out}$  and  $C_{G,in}$  are the outlet and inlet  $\text{O}_2$  concentrations ( $\text{g O}_2 \text{m}^{-3}$ ) of the packed bed, respectively;  $K_L$  is the global liquid mass transfer coefficient ( $\text{m h}^{-1}$ );  $a$  is the interfacial area ( $\text{m}^2 \text{m}^{-3}$ );  $V_C$  is the packing volume ( $\text{m}^3$ ) and  $H$  is the dimensionless gas-liquid Henry coefficient.

A full factorial design ( $3^2$ ) was performed for  $Q$  (1, 3 and  $5.2 \text{ m}^3 \text{h}^{-1}$ ) and  $Q_L$  (1, 2 and  $3 \text{ m}^3 \text{h}^{-1}$ ). The global mass transfer coefficient was determined in both flow modes (co- and counter-current), thus, notice that  $C_{L,out}$ ,  $C_{L,in}$ ,  $C_{G,out}$  and  $C_{G,in}$  corresponded either to the top or bottom concentrations of the packed bed depending on the flow mode under analysis.

### 2.3. Co-current and counter-current flow operation mode

The operating conditions of the BTF are summarized in Table 1. The effect of increasing  $\text{H}_2\text{S}$  inlet loads (IL) was assessed under counter-current flow mode (Fig. 1a) and co-current flow mode (Fig. 1b) during 297 and 63 days, respectively. The operating conditions were maintained constant for at least for 24 h and 0.75 h in the long- and short-duration experiments, respectively. Under co-current flow the effect of increasing IL was carried out through short-time experiments.

In both operation flow modes, the nitrate concentrate solution was added automatically using a feeding control strategy based on the oxidation-reduction potential (ORP) measurement (Almenglo et al., 2016). In short, a fixed volume of the liquid sump was purged when an ORP set-point of  $-365 \text{ mV}$  was reached and automatically replaced with IW. Such volume was defined as ten times the volume of the nitrate concentrate solution added.

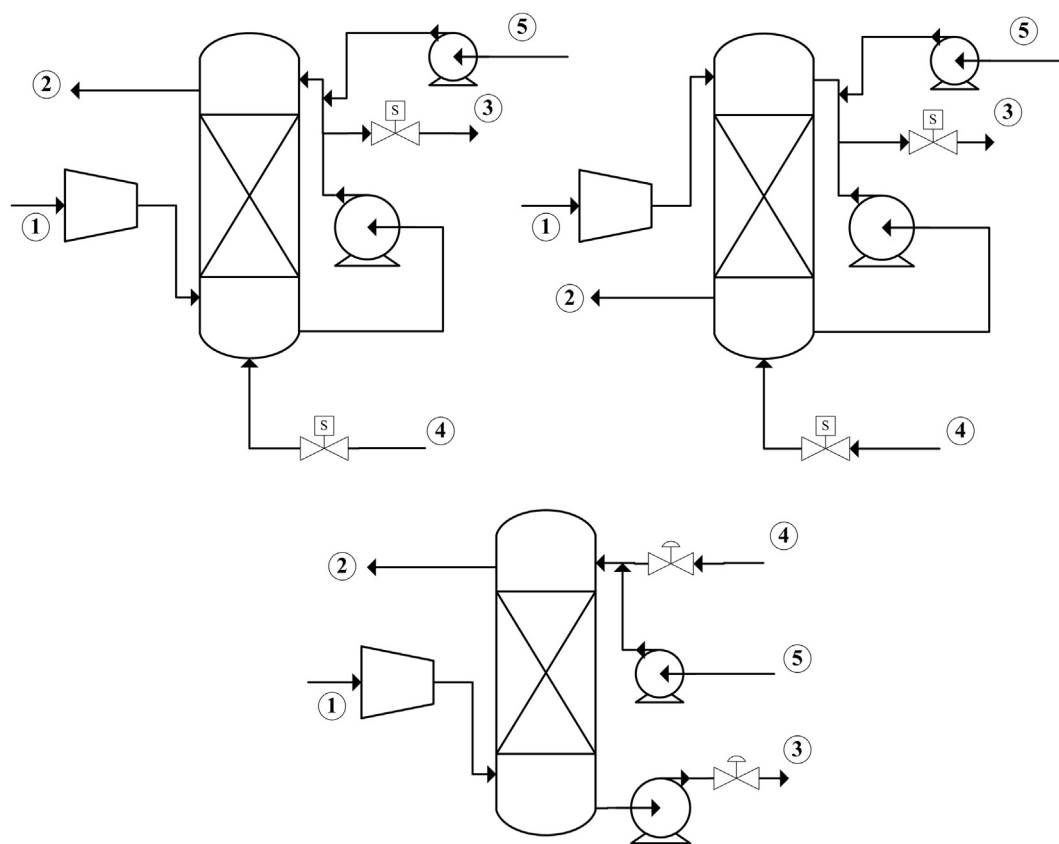
### 2.4. Elemental sulfur de-accumulation experiments

Sulfur mass balances were carried out under counter-current operation to assess the mass of elemental sulfur removed in the BTF.  $Q$  and  $Q_L$  were kept constant at  $3 \text{ m}^3 \text{h}^{-1}$ . Four experiments of 18 h each were carried out at different maximum nitrate concentrations of 299.8, 149.2, 69.3 and  $9.1 \text{ mg N-NO}_3^- \text{L}^{-1}$ . First, an average inlet  $\text{H}_2\text{S}$  concentration of  $5.29 \pm 0.68 \text{ g S m}^{-3}$  was fed, which corresponded to N:S ratios consumed ranging from 0.96 to  $1.25 \text{ mol-N mol-S}^{-1}$ . Later, a period of 136 h without biogas supply was decided in order to reduce the elemental sulfur accumulation in the packed bed.

**Table 1**

Operating conditions during long- (24 h) and short-duration (0.75 h) experiments along the experimental period under study.

Flow mode	Counter-current		Co-current	
Duration <sup>a</sup> (h)	24	0.75	0.75	
Days	282–296	297	298 and 360	
Q (m <sup>3</sup> h <sup>-1</sup> )	1–5.2		1–4.5	
Q <sub>L</sub> (m <sup>3</sup> h <sup>-1</sup> )	3			
[N-NO <sub>3</sub> ] (mg N-NO <sub>3</sub> L <sup>-1</sup> )	92–221 mean: 143 ± 37	950–1269 mean: 1128 ± 119	1198–1349 mean: 1283 ± 75	1158–1446 1284 ± 112
[H <sub>2</sub> S] inlet (ppmv)	4490 ± 360	4236 ± 45	4031 ± 60	4258 ± 81
[S-SO <sub>4</sub> <sup>2-</sup> ] (mg S-SO <sub>4</sub> <sup>2-</sup> L <sup>-1</sup> )	7600 ± 920	2540 ± 320	3430 ± 320	5115 ± 100
[S <sup>2-</sup> ] (mg S <sup>2-</sup> L <sup>-1</sup> )	1.2 ± 0.8	1.8 ± 1	24.5 ± 12.1	7.4 ± 2.6

<sup>a</sup> Length of the experimental period under constant conditions.**Fig. 1.** 1. Biogas inlet, 2. Biogas outlet, 3. Water purge, 4. Industrial water, 5. Nitrate concentrate solution.

### 2.5. Single-pass, continuous liquid flow operation

During a period of 14 days (days 402–415) under counter-current flow, a single-pass of IW was decided. Thus, the BTF was continuously fed with IW from the top of the column and without recirculation of the water phase (Fig. 1c). The nitrate concentrate solution was mixed with the IW stream. The IW flow rate was 1.7 m<sup>3</sup> h<sup>-1</sup> while the H<sub>2</sub>S ILs were 41.7 ± 5.3, 82.9 ± 7.3 and 115.4 ± 0.3 g S m<sup>-3</sup> h<sup>-1</sup>. Nitrate mass flow rates of 21.8 ± 2.3 and 69.8 ± 4.3 g N-NO<sub>3</sub> h<sup>-1</sup> were tested at each IL.

### 2.6. Microbial diversity analysis

bTEFAP was selected as the sequencing approach to assess microbial diversity of three biomass samples taken during the

operation of the BTF. Samples Ca-A (bottom of the BTF) and Ca-B (top of the BTF) were sampled on day 343, which corresponded to day 46 of the co-current flow period with liquid recirculation. Ca-C was taken from the bottom of the packed bed on day 415, after 14 days under operation in counter-current flow mode with single-pass, continuous IW supply.

Biomass from PUF was liberated by squeezing and mechanical agitation of PUF cubes. Then, samples were concentrated by centrifugation (8000 rpm, 10 min) and the supernatant was discarded to form the pellet. Samples were stored at -20 °C for further processing. DNA was extracted from 0.1 g of pellets with PowerBiofilm™ DNA Isolation kit (MoBio Laboratories, USA). The quality and concentration checking of extracted DNA, libraries preparation and PCR emulsion and reaction for sequencing were performed as described in Montebello et al. (2013). PCR primers 341F and 907R'

were used. Tags used for sequence identification are shown in Table S1. Sequencing was performed on a FLX+ 454 Roche platform at Research and Testing Laboratory (RTL) (Texas, USA). Raw data provided by RTL was re-processed as described in section SM-2. All analyses were assessed in the Ribosomal Database Project (RDP). Details of the number of sequence reads filtered at each stage are provided in Table S1.

Based upon data of sequence identity percentage, sequences were classified at the appropriate taxonomic level as reported in Montebello et al. (2013). Data obtained provided relative abundance within and among individual samples. Relative abundance data at genera level were plotted to analyze the diversity profile. Phylogenetic distances were used for phylogenetic trees construction (>bootstrap 80%). The Shannon diversity index ( $H'$ ) coupled to the equitativity index ( $E'$ ) and the *Chao1* index were calculated based on the constructed clusters at 3% divergence. Indices of biological diversity calculated for both libraries (Table S2) indicated that libraries were comparable in terms of abundance percentages and that good coverage of diversity was reached. Also, rarefaction curves (Fig. S1) demonstrated the proper coverage of the libraries constructed.

### 3. Results and discussion

#### 3.1. Mass transfer coefficient determination

The global mass transfer coefficient was determined according to equation (3) with a linear correlation coefficient ( $r^2$ ) above 0.98. The  $K_{La}$  values obtained in co-current and counter-current mode ranged from 20.0 to 52.2 and from 17.9 to 51.9  $h^{-1}$ , respectively (Table 2). Therefore, no significant differences were found between co- and counter-current mass transfer coefficients. The most influencing factor on  $K_{La}$  was the liquid flow rate. Fig. 2 shows the mean  $K_{La}$  for the three liquid flow rates evaluated and the theoretical estimations using well-known empirical correlations (Dorado et al., 2009). The Van Krevelen and Hoftijzer correlation provided the closest estimation of  $K_{La}$  to the experimental data. The  $K_{La}$  values for the Onda and the Shulman correlations were 2.5 and 8 times higher, respectively, than the experimental ones.

The  $K_{La}$  depends on many factors such as the effective surface area of the packing material, gas and liquid velocities, gas distribution, stagnant zones, etc (Kraakman et al., 2011). A wide range of  $K_{La}$  between 15 and 300  $h^{-1}$  have been reported for PUF (Estrada et al., 2014; Kim and Deshusses, 2008). For instance, Kim and Deshusses (2008) obtained  $K_{La}$  between 30 and 35  $h^{-1}$  at a trickling liquid velocity (TLV) of 12  $m h^{-1}$ ,  $Q/Q_L$  ratio between 8.3 and 391, empty bed residence time (EBRT) between 0.031 and 1.44 s, and a height-to-diameter (H/D) ratio of 2.67. Estrada et al. (2014) found a  $K_{La}$  of 130  $h^{-1}$  at larger EBRT (120 s) and lower TLV (5  $m h^{-1}$ ), corresponding to a  $Q/Q_L$  ratio of 4.8 and an H/D ratio of

**Table 2**  
 $K_{La}$  obtained in co- and counter-current flows.

		Co-current			Counter-current		
$Q (m^3 h^{-1})$	$Q_L (m^3 h^{-1})$	$T^a (^\circ C)$	$K_{La} (h^{-1})$	$r^2$	$T^a (^\circ C)$	$K_{La} (h^{-1})$	$r^2$
1	1	21	20.0	0.994	23	17.9	0.991
3		21	21.9	0.989	20	20.5	0.997
5		22	22.5	0.998	23	20.2	0.996
1	2	21	38.1	0.991	23	32.4	0.994
3		23	37.3	0.996	22	33.2	0.998
5		22	37.2	0.990	22	34.4	0.980
1	3	23	52.2	0.994	23	51.9	0.996
3		22	50.4	0.987	22	50.2	0.994
5		22	50.7	0.995	23	50.1	0.990

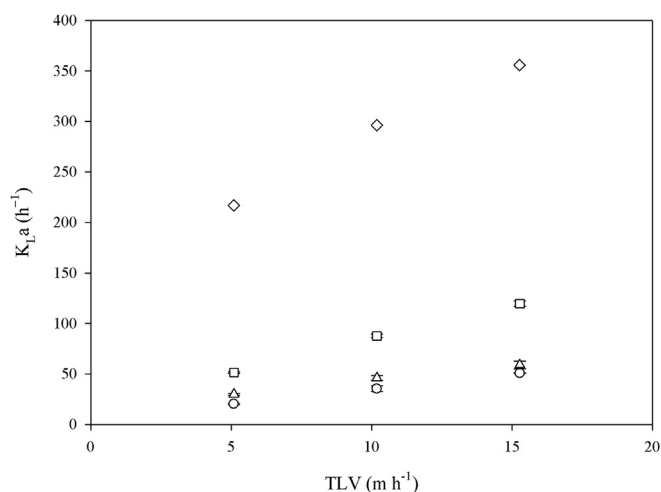


**Fig. 2.** Comparison between experimental  $K_{La}$  (circles) and  $K_{La}$  calculated by the Van Krevelen & Hoftijzer (triangles), Onda (squares) and Shulman (diamonds) correlations.

9.95. In our study, under counter-current flow, the  $K_{La}$  values were between 32.4 and 34.4  $h^{-1}$  for TLV of 10  $m h^{-1}$ ,  $Q/Q_L$  ratio between 0.5 and 2.5, EBRT between 120 and 600 s and an H/D ratio of 1.70. Our results were close to Kim and Deshusses (2008), although there were significant differences related to the EBRT. Our  $K_{La}$  was much lower compared to Estrada et al. (2014). At a TLV of 5  $m h^{-1}$  the  $K_{La}$  ranged from 17.9 to 20.5  $h^{-1}$ . This large discrepancy was attributed to the different H/D ratio affecting the liquid distribution efficiency, stagnant zones and the effective surface.

#### 3.2. Performance under co- and counter-current flow operation modes

During counter-current flow operation, the  $H_2S$  IL was varied from 33 to 193  $g S m^{-3} h^{-1}$ . As shown in Fig. 3, long- and short-duration experiments showed a very similar performance of the BTF, indicating that experiments carried out during 0.75 h were adequate to reach steady-state conditions. The maximum elimination capacity ( $EC_{max}$ ) was 140  $g S m^{-3} h^{-1}$  (RE 84%) and the critical elimination capacity ( $EC_{crit}$ ) was 56  $g S m^{-3} h^{-1}$  (RE 98%).

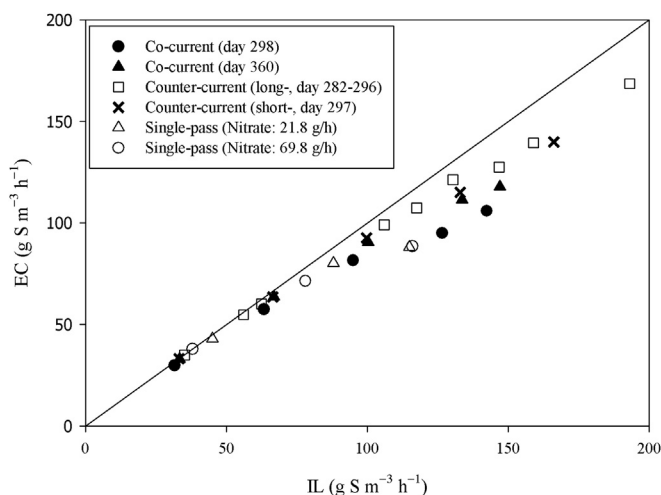


**Fig. 3.** Performance data for the anoxic BTF in terms of  $H_2S$  Elimination Capacity (EC) under different operating conditions. Long- and short-state for long-duration and short-duration type of experiments.

Similar  $EC_{max}$  ( $100\text{--}140\text{ gS m}^{-3}\text{ h}^{-1}$ ) were obtained by Montebello et al. (2014) and Fernández et al. (2014) ( $EC_{max} = 169\text{ gS m}^{-3}\text{ h}^{-1}$ ) at lab-scale. Under co-current flow mode, IL was varied from 32 to  $147\text{ gS m}^{-3}\text{ h}^{-1}$  (Fig. 3). The  $EC_{max}$  was  $118\text{ gS m}^{-3}\text{ h}^{-1}$  (RE 80%) while the  $EC_{crit}$  was  $33\text{ gS m}^{-3}\text{ h}^{-1}$  (RE 99%). Taking into consideration that no significant differences were found in G-L mass transport between both flow modes, the slightly worst performance under co-current flow mode was attributed to the redistribution of the biomass activity along the packed bed during the co-current flow mode. The biomass and elemental sulfur redistribution were confirmed by visual inspections (Fig. S2). Under counter-current flow, the biomass growth was higher in the bottom part of the packed bed where the higher  $H_2S$  concentration was found. Biofilm growth rates are usually higher near the gas inlet than the gas outlet (Yang et al., 2010). Moreover, under counter-current flow, the larger nitrate availability is on top of the bed while at the bed bottom the lowest N:S ratio is found, which leads to the highest elemental sulfur production rate because the elemental sulfur production is directly related to the N:S ratio. In this BTF, N:S molar ratios between  $0.34$  and  $1.74\text{ mol-N mol-S}^{-1}$  were tested with a sulfate production between 8% and 95%, respectively (Almenglo et al., 2016). Hence, an alternate operation between counter-current and co-current flow modes promotes the redistribution in the concentration of biomass and elemental sulfur along the bed, which allows a decrease in the pressure drop and, therefore, a larger life span of the packed bed between maintenance episodes.

### 3.3. Elemental sulfur de-accumulation experiments

In terms of sulfur mass balance, the mean sulfate concentration was  $5950 \pm 474\text{ gS-SO}_4^{2-}\text{ m}^{-3}$  and the  $H_2S$  RE in the four experiments ranged between 87 and 92%. Therefore, no influence in the RE was found by the variation in the maximum nitrate concentration supplied. The N:S ratio fed ranged from  $0.96$  to  $1.25\text{ mol-N mol-S}^{-1}$ . Under this conditions, the sulfate selectivity, which is defined as the percentage of sulfate produced with respect to the  $H_2S$  removed, ranged from  $47 \pm 0.05$  to  $57 \pm 0.06\%$ , respectively. Similar values were found by Fernández et al. (2014) in a lab-scale BTF. At a N:S ratio of  $1\text{ mol-N mol-S}^{-1}$  they found a 60% of sulfate produced.

During the first 360 days (Table 1) the biogas supply was stopped 7 times for a period between 3 and 7 days (323 days on and 37 days off). The larger period with biogas supply was 127 days ( $IL\ 91.5\text{ gS m}^{-3}\text{ h}^{-1}$ ) followed by a shutdown period of 7 days. Based on the sulfate production along this period, an elemental sulfur de-accumulation rate of  $59.1\text{ gS m}^{-3}\text{ h}^{-1}$  was determined. Similar elemental sulfur de-accumulation rates between 44 and  $100\text{ gS m}^{-3}\text{ h}^{-1}$  have been measured in aerobic BTF (Montebello et al., 2014). Therefore, biogas supply cuts are also a feasible strategy to reduce undesired elemental sulfur accumulation in anoxic BTFs.

### 3.4. Performance of the BTF under a single-pass liquid flow mode

As shown in Fig. 3, under a single-pass configuration the  $EC_{crit}$  ( $37.9\text{ gS m}^{-3}\text{ h}^{-1}$ , RE 99%) and  $EC_{max}$  ( $88.4\text{ gS m}^{-3}\text{ h}^{-1}$ ) were lower than the results obtained under co- and counter-current operation with liquid recycle because of the lower liquid flow rate used ( $1.7\text{ m}^3\text{ h}^{-1}$ ), which hindered  $H_2S$  mass transfer. In fact, no differences in terms of RE were found between both nitrate flow rates tested.

A comparison between the ratios  $N:S_{consumed}$  and  $N:S_{fed}$  for both nitrate flow rates showed marked differences (Fig. 4). The  $N:S_{fed}$  and  $N:S_{consumed}$  were  $2.44\text{--}20.55$  and  $0.15\text{--}4.72\text{ mol-N mol-S}^{-1}$ , respectively, that varied as a function of the  $H_2S$  IL. A  $N:S_{consumed}$

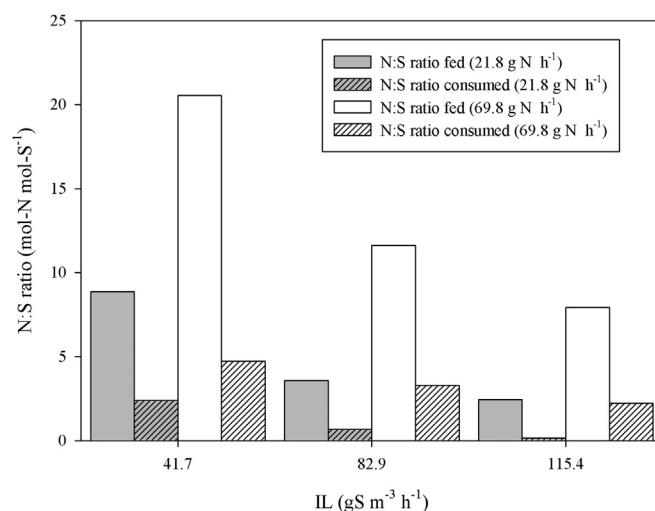


Fig. 4. Influence of the mass flow rate of nitrate supplied on the N:S ratio fed and consumed at different  $H_2S$  IL during single-pass liquid flow mode.

decrease was encountered as the  $H_2S$  IL increased. Consequently, a large amount of nitrate was wasted, mainly at low  $H_2S$  IL, and therefore the use of a single-pass of IW was not an efficient operation mode. It is worth mentioning that at  $69.8 \pm 4.3\text{ g N-NO}_3^- \text{ h}^{-1}$  the ratio  $N:S_{consumed}$  ( $2.23\text{--}4.72\text{ mol-N mol-S}^{-1}$ ) was very high compared to reported autotrophic denitrification ratios (Mora et al., 2015). As detailed in section 3.5, heterotrophic denitrifiers were responsible of such high  $N:S_{consumption}$ .

### 3.5. Microbial diversity analysis

Three amplicon libraries, namely Ca-A, Ca-B and Ca-C, were constructed. Samples Ca-A and Ca-B allowed the comparison of the bacterial diversity on top and bottom of the packed bed during the co-current flow mode. Sample Ca-C showed the impact of a single-pass flow of IW instead of a recirculating solution. A total of 46126 sequence reads were obtained while 25516 were annotated as 5013 sequence reads for Ca-A, 5855 sequence reads for Ca-B and 14648 sequence reads for Ca-C. In the data set 5 phyla, 14 classes, 33 families and 43 genera were estimated for Ca-A; 4 phyla, 12 classes, 30 families and 37 genera were estimated for Ca-B; and 7 phyla, 28 classes, 84 families and 153 genera were estimated for Ca-C. Quality check data (Table S1) demonstrates the complexity to assign identity. While Ca-A was successfully identified due to the predominance of a single taxon, only 25% of the sequences were annotated to genera in Ca-C due to a larger diversity, to the limited coverage of the sequence database and to the amplicons length (440 nt on average). Because of the large coverage of the bTEFAP, relative abundance thresholds of OTUs identified were set at 0.1% in all libraries, which corresponded to a minimum of 10 reads per sequence. Lu et al. (2014) reported similar limitations of the 16S sequences databanks for denitrifying species. Regarding community structure, lower *Chao1*, *Shannon (H')* and *Equitativity (E)* indexes for Ca-A (Table S2) showed that the community of sample Ca-A was much more specialized and had a much less uniform distribution of the sequences compared to that of Ca-B and Ca-C. According to literature (Cabrol and Malhautier, 2011; Cabrol et al., 2012, 2009), results reflected a large equilibrium in terms of species diversity, which was essential for the community to resist transient, punctual environmental changes.

Distribution of phyla and families in each sample are shown in Fig. 5 while the distribution of classes is provided in Fig. S4.

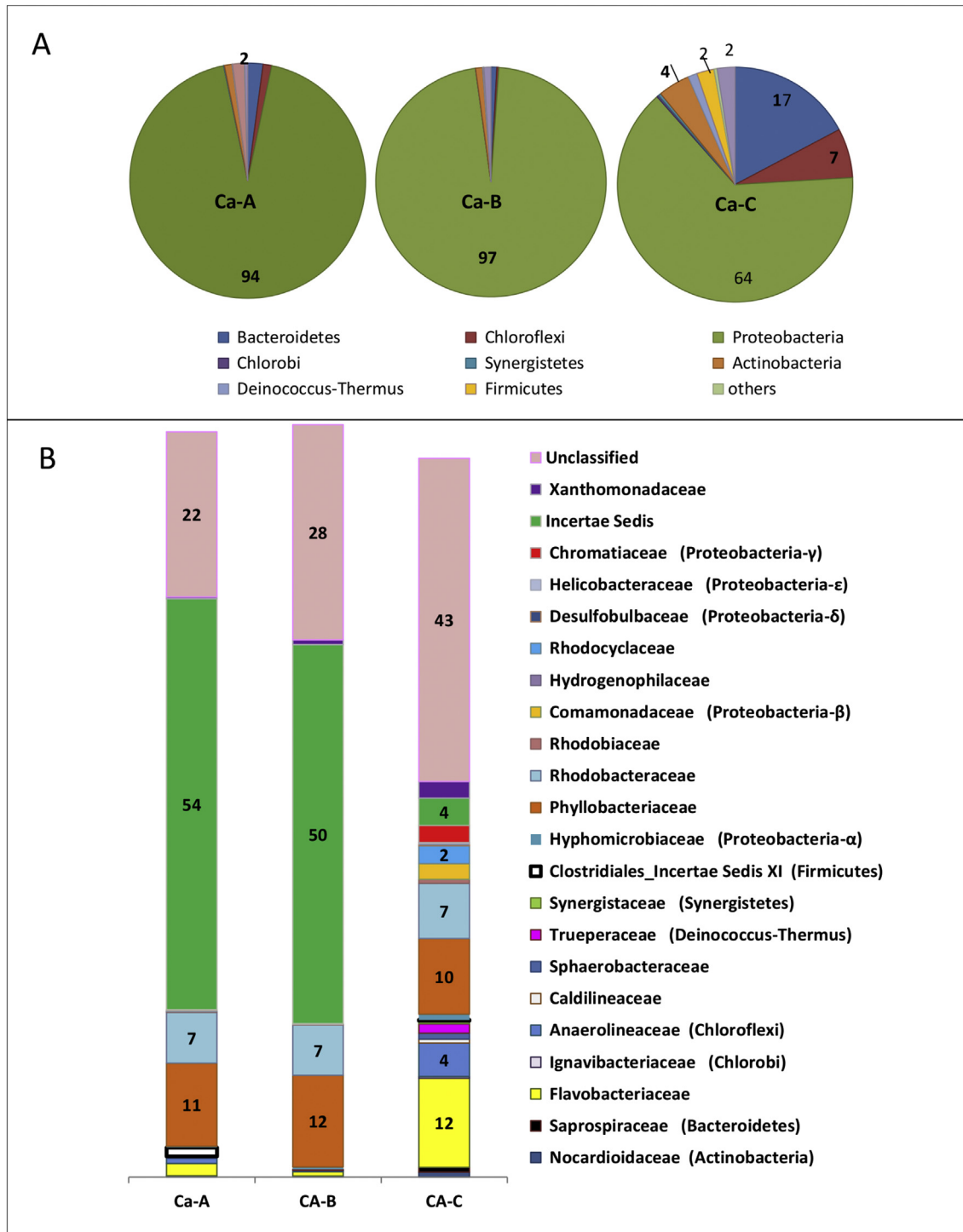


Fig. 5. Relative abundances at a) phylum and b) family level of Ca-A, Ca-B and Ca-C samples.

Proteobacteria markedly predominated in all samples (64–97%) while Bacteroidetes and Chloroflexi raised up to 17 and 7%, respectively, only in sample Ca-C. Among Proteobacteria,  $\gamma$ -proteobacteria class had a relative abundance above 70% in Ca-A and Ca-B, which dropped down to 35% in Ca-C. Class  $\alpha$ -proteobacteria was also relevant in all samples, accounting for 20–24% in all samples.

A closer look to samples Ca-A and Ca-B allowed explaining the impact of the operation in co-current flow on the distribution of

biomass between the top and the bottom of the packed bed assuming that the time span between the switch to co-current operation and the sampling episode was enough. Relative abundances at family level (Fig. 5, Table 3) showed that most of the predominant taxa in Ca-A and Ca-B corresponded either to unclassified (22 and 28% in Ca-A and Ca-B, respectively) and to *Incertae Sedis* (54 and 50% in Ca-A and Ca-B, respectively), the latter corresponding to uncompleted taxonomic classification (Kuever and Widdel, 2006). Identity of *unclassified* species was

**Table 3**  
Phylogenetic classification and relative abundance of *genus*. Underlined names correspond to known denitrifying *genus*.

Class	Phylogenetic classification		Abundance						
	Family	Assigned identity	Ca-A		Ca-B		Ca-C		
			N	(%)	N	(%)	N	(%)	
$\alpha$ -proteobacteria	Phyllobacteriaceae	<i>Hoeflea</i>	406	8.1	487	8.3	520	3.5	
		<i>Nitratireductor</i>	41	0.8	35	0.6	161	1.1	
		Phyllobacteriaceae (uncl. genus)	99	2.0	176	3.0	733	5.0	
	Rhizobiaceae	Rhizobiales (uncl. family)	45	0.9	118	2.0	349	2.4	
	Rhodobacteraceae	<i>Paracoccus</i>	73	1.5	83	1.4	291	2.0	
		<i>Roseovarius</i>	40	0.8	13	0.2	88	0.6	
		<i>Rhodobacter</i>		<0.1		<0.1	83	0.6	
		Rhodobacteraceae (uncl. genus)	197	3.9	266	4.5	561	3.8	
	Rhodobiaceae	<i>Tepidamorphus</i>		<0.1		<0.1	73	0.5	
		$\alpha$ -proteobacteria (uncl. family)	29	0.6	173	3	233	1.6	
$\beta$ -proteobacteria	Comamonadaceae	<i>Simplicispira</i>		<0.1		<0.1	8	0.1	
		Comamonadaceae (uncl. genus)		<0.1		<0.1	272	1.9	
	Rhodocyclaceae	Rhodocyclaceae (uncl. genus)		<0.1		<0.1	185	1.3	
		<i>Thauera</i>		<0.1		<0.1	116	0.8	
		Burkholderiales (uncl. family)		<0.1		<0.1	25	0.2	
		$\beta$ -proteobacteria (uncl. family)		<0.1		<0.1	61	0.4	
	$\delta$ -proteobacteria	Desulfobulbaceae	Desulfobulbaceae (uncl. genus)		<0.1		<0.1	27	0.2
		<i>Sulfurovum</i> <sup>2</sup>		<0.1		<0.1	25	0.2	
	$\epsilon$ -proteobacteria	Helicobacteraceae	Chromatiaceae (uncl. genus)		<0.1		<0.1	307	2.1
	$\gamma$ -proteobacteria	Chromatiaceae	Chromatiales (uncl. family)		<0.1		<0.1	35	0.2
<i>Sedimenticola</i>			2480	49.5	2589	44.2	533	3.6	
<i>Incertae Sedis</i>		<i>Incertae Sedis</i> (uncl. genus)	241	4.8	341	5.8	639	4.4	
		<i>Marinicella</i>		<0.1		<0.1	74	0.5	
		Xanthomonadaceae	Xanthomonadaceae (uncl. genus)	12	0.2	35	0.6	310	2.1
		$\gamma$ -proteobacteria (uncl. family)	844	16.8	958	16	2948	20.1	
		Proteobacteria (uncl. class)	53	1.1	283	4.8	170	1.2	
Actinobacteria		Nocardioideae	Actinomycetales (uncl. family)	34	0.7	28	0.5	321	2.2
		<i>Nocardioides</i>		<0.1		<0.1	69	0.5	
Flavobacteria		Flavobacteriaceae	Flavobacteriaceae (uncl. genus)	81	1.6	30	0.5	1718	11.7
	Flavobacteriales (uncl. family)		<0.1		<0.1	79	0.5		
Sphingobacteria	Saprosiraceae	Saprosiraceae (uncl. genus)		<0.1		<0.1	83	0.6	
	Bacteroidetes (uncl. phylum)		<0.1		<0.1	458	3.1		
Anaerolineae	Anaerolineaceae	<i>Bellilinea</i>		<0.1		<0.1	14	0.1	
	Anaerolineaceae (uncl. genus)		32	0.6	6	0.1	597	4.1	
Caldilineae	Caldilineaceae	<i>Caldilinea</i>		<0.1		<0.1	80	0.5	
Ignavibacteria	Ignavibacteriaceae	<i>Ignavibacterium</i>		<0.1		<0.1	38	0.3	
Thermomicrobia	Sphaerobacteraceae	<i>Sphaerobacter</i>		<0.1		<0.1	114	0.8	
	Chloroflexi (uncl. class)			<0.1		<0.1	134	0.9	
Deinococci	Trueperaceae	<i>Truepera</i>		<0.1		<0.1	182	1.2	
Clostridia	<i>Incertae Sedis XI</i>	<i>Tissierella</i>	31	0.6		<0.1		<0.1	
		Clostridiales (uncl. family)	27	0.5	0	0	34	0.2	
		Firmicutes (uncl. class)		<0.1		<0.1	93	0.6	
		Bacteria (uncl. phylum)	22	0.4	57	1	357	2.4	
Others			226	4.6	177	3.1	1450	9.9	
TOTAL			5013	100	5855	100	14648	100	

(uncl.): unclassified, N: number of sequences assigned.

investigated for the predominant class  $\gamma$ -proteobacteria through Blast and ClustalW, via MEGA6. Clusters CaSp01, CaSp02 and CaSp03 were investigated (Fig. S1). Clusters CaSp01 and 02 were related with a species close to *Sedimenticola*. *Sedimenticola* sp. has been found taking over the *Sulfurimonas denitrificans* in anammox process as the dominant sulfide oxidizer (Russ et al., 2014). Lower similarity was found with other bacteria related with the S and N cycle (*Methylobacter*, *Thiohalomonas*, *Thiohalocapsa*, *Thioalkalispira*, *Thiohalophilus*). Therefore, *Sedimenticola* was assumed to play the main desulfurizing role in both parts of the reactor. *Sedimenticola* type bacteria has attracted great interest because of their metabolic versatility and potential for autotrophic denitrification to form extracellular S<sup>0</sup>. Moreover, chemolithoautotrophic growth also occurs with tetrathionate and elemental sulfur (Flood et al., 2015b). After studies of the whole genome of some strains, the phylogenetic identity of this new genus began to clear. In literature, the description of only three species is found: *Sedimenticola selenatireducens* (Narasimgarao and Häggblom, 2006), *Sedimenticola* sp

(Russ et al., 2014), and *Sedimenticola thiotaurini* (Flood et al., 2015a, 2015b), which are all SO-NR bacteria. The ability of *Sedimenticola* sp. for autotrophic denitrification was confirmed in an anammox reactor. Authors found a gradual increase in species abundance over time and a marked predominance over other denitrifying proteobacteria classes (Russ et al., 2014). This behavior matches what we observed in our anoxic BTF. Subsequently, gene distribution studies confirmed their metabolic potential. The genome encoded the Sox pathway (soxABXYZ) and an almost complete denitrification pathway with genes for nitrate and nitrite reductase and nitrous oxide reductase detected in the genome assembly (Flood et al., 2015b). The information collected in literature allowed us attributing the leading role of the autotrophic denitrification in the anoxic BTF to this bacteria.

It is worth mentioning that Rhodobacteraceae- $\alpha$  (7% in both samples) and Phyllobacteriaceae- $\alpha$  (11 and 12% in Ca-A and Ca-B, respectively) were the most abundant identified families in samples Ca-A and Ca-B. Both families contain genera related to the N

and S cycles. In Phyllobacteriaceae- $\alpha$ , almost 8% of sequences were related to *Hoeflea* and 1% to *Nitratireductor* in both samples. In Rhodobacteraceae- $\alpha$ , around 1.5% were related with *Paracoccus* and 1.0% of reads in Ca-A were related to *Roseovarius* (0.2% in Ca-B). In addition, Blast sequences of the *unclassified* set were related to *Paracoccus* (*Paracoccus* sp, *P. denitrificans*, or *P. versatus*  $\leq$  97% similarity). The typical versatility of *Paracoccus* species and the physiology of *Roseovarius* (heterotrophic) suggested that family Rhodobacteraceae participated in heterotrophic denitrification. Blast results for  $\alpha$ -proteobacteria (*uncl. family*) also showed similarity with *P. denitrificans* (92% similarity) and *Nitrobacter winogradskyi* (70%), quimiolitotrophic species of the N cycle able to use nitrite (Lu et al., 2014). Based on these results it is assumed that  $\alpha$ -proteobacteria was enriched because of its capability to denitrify heterotrophically, which competed with SO-NR species for the electron acceptor, either nitrate or nitrite.

Overall, operation in co-current mode favored the development of generalist species in the lower part of the BTF, while more specialized communities developed in the upper part of the packed bed. In the upper part of the BTF, which is close to the inlet gas and nitrate supply (sample Ca-A), the high H<sub>2</sub>S concentration and nitrate availability promoted the growth of autotrophic SO-NR species. In the lower part of the reactor (sample Ca-B), where nitrate is scarce, other N species such as nitrite, NO<sub>2</sub> or N<sub>2</sub>O probably lead to a wider diversity with more generalist species.

Comparison of samples between the period of operation under recirculating co-current flow (samples Ca-A and Ca-B) with the period of operation in single-pass, counter-current flow without liquid recirculation (sample Ca-C) showed large changes in the structure of the communities. Main changes at phylum level (Fig. 5) were found in Proteobacteria, that reduced its relative abundance from 94 to 64%; in Bacteroidetes, which increased from 2 to 17%; and in Chloroflexi, which also increased from 1 to 7%. At class level (Fig. S4), main changes were found in the increase in  $\beta$ -Proteobacteria up to 5% and the decrease of  $\gamma$ -Proteobacteria from 72 to 33%. At family level (Fig. 5), two main changes were found: 1) the dramatic reduction of *Incertae Sedis*- $\gamma$  sequences from 54% in Ca-A to 8% in Ca-C, and 2) the increase of Flavobacteriaceae from 2 to 12%. At genera level (Table 3) results show a larger redistribution of sequences reads in Ca-C indicating a more complex community structure. Among main changes, *Sedimenticola* abundance was reduced from 50 to 4%, while Flavobacteriaceae (*uncl. genus*) increased from around 1 to 12%. Analysis of similarity at species level corroborated the competence between heterotrophic  $\alpha$ -proteobacteria with quimiolitotrophic  $\gamma$ -proteobacteria (data not shown). It is worth mentioning that the autotrophic community in Ca-A reached 70% of sequence reads while only 33% was accounted in Ca-C, which correlated well with the lower performance of the BTF in the period without water recirculation.

Overall, the presence of non SO-NR, opportunistic heterotrophic bacteria correlated well with the results obtained in previous sections regarding the large production of elemental sulfur at N:S ratios were mostly sulfate production was expected. This fact has practical implications in the sense that a larger nitrate supply is needed to avoid elemental sulfur production.

#### 4. Conclusions

Anoxic biofiltration of biogas is a reliable technology for biogas desulfurization. The higher elimination capacity (140 gS m<sup>-3</sup> h<sup>-1</sup>) was reached under counter-current flow. A better distribution of biomass and elemental sulfur was observed (visual inspection) switching to co-current flow, which is envisioned as a strategy to increase the carrier lifetime. The elemental sulfur accumulation (47–57%) into the carrier could be reduced by switching off the

biogas feeding while keeping the nitrate addition to the BTF. *Sedimenticola* was the main desulfurizing bacteria. However, under continuous flow mode *Sedimenticola* was reduced from 50 to 4% and the elimination capacity was reduced. Heterotrophic denitrifying species found implies some competition for nitrate with specialized, autotrophic denitrifiers.

#### Acknowledgements

The Spanish government (MINECO) provided financial support through the project CTM2012-37927-C03-01/FEDER and CTM2012-37927-C03-03/FEDER. Authors thank to WWTP “Bahía Gaditana” for offering their facilities and resources. T. Bezerra wants to thank her funding to the programs of Conselho nacional de Desenvolvimento Científico e Tecnológico- Coordenação de Aperfeiçoamento de Pessoal de Nível Superior (CNPq/CAPES) from the Brazil government.

#### Appendix A. Supplementary data

Supplementary data related to this article can be found at <http://dx.doi.org/10.1016/j.chemosphere.2016.05.016>.

#### References

- Almenglo, F., Ramírez, M., Gómez, J.M., Cantero, D., 2016. Operational conditions for start-up and nitrate-feeding in an anoxic biotrickling filtration process at pilot scale. *Chem. Eng. J.* 285, 83–91.
- Cabrol, L., Malhautier, L., 2011. Integrating microbial ecology in bioprocess understanding: the case of gas biofiltration. *Appl. Microbiol. Biotechnol.* 90, 837–849.
- Cabrol, L., Malhautier, L., Poly, F., Lepeuple, A.S., Fanlo, J.L., 2009. Shock loading in biofilters: impact on biodegradation activity distribution and resilience capacity. *Water Sci. Technol.* 59, 1307.
- Cabrol, L., Malhautier, L., Poly, F., Roux, X. Le, Lepeuple, A.S., Fanlo, J.L., 2012. Resistance and resilience of removal efficiency and bacterial community structure of gas biofilters exposed to repeated shock loads. *Bioresour. Technol.* 123, 548–557.
- Cheng, Z., Lu, L., Kennes, C., Yu, J., Chen, J., 2016. Treatment of gaseous toluene in three biofilters inoculated with fungi/bacteria: microbial analysis, performance and starvation response. *J. Hazard. Mater.* 303, 83–93.
- Clesceri, L.S., Greenberg, A.E., Eaton, A.D., 1999. *Standard Methods for the Examination of Water and Wastewater*, twentieth ed. American Public Health Association, Washington DC.
- Dorado, A.D., Rodríguez, G., Ribera, G., Bonsfills, A., Gabriel, D., Lafuente, J., Gamisans, X., 2009. Evaluation of mass transfer coefficients in biotrickling filters: experimental determination and comparison to correlations. *Chem. Eng. Technol.* 32, 1941–1950.
- Estrada, J.M., Dudek, A., Muñoz, R., Quijano, G., 2014. Fundamental study on gas-liquid mass transfer in a biotrickling filter packed with polyurethane foam. *J. Chem. Technol. Biotechnol.* 89, 1419–1424.
- Fernández, M., Ramírez, M., Gómez, J.M., Cantero, D., 2014. Biogas bio-desulfurization in an anoxic biotrickling filter packed with open-pore polyurethane foam. *J. Hazard. Mater.* 264, 529–535.
- Flood, B.E., Jones, D.S., Bailey, J.V., 2015a. Complete genome sequence of *Sedimenticola thiotaurini* strain SIP-g1, a polyphosphate- and polyhydroxyalkanoate-accumulating sulfur-oxidizing gammaproteobacterium isolated from salt marsh sediments. *Genome. announc.* 3, e00671–e00715.
- Flood, B.E., Jones, D.S., Bailey, J.V., 2015b. *Sedimenticola thiotaurini* sp. nov., a sulfur-oxidizing bacterium isolated from salt marsh sediments, and emended descriptions of the genus *Sedimenticola* and *Sedimenticola selenitireducens*. *Int. J. Syst. Evol. Microbiol.* 65, 2522–2530.
- Kim, S., Deshusses, M.A., 2008. Determination of mass transfer coefficients for packing materials used in biofilters and biotrickling filters for air pollution control. 1. Experimental results. *Chem. Eng. Sci.* 63, 841–855.
- Kraakman, N.J., Rocha-Rios, J., van Loosdrecht, M.C., 2011. Review of mass transfer aspects for biological gas treatment. *Appl. Microbiol. Biotechnol.* 91, 873–886.
- Kuever, J.F.A.R., Widdel, F., 2006. *Bergey's manual of systematic bacteriology*, the proteobacteria. Part C, the alpha-, beta-, delta-, and epsilonproteobacteria. In: *Bergey's Manual of Systematic Bacteriology*, the Proteobacteria. Part C, the Alpha-, Beta-, Delta-, and Epsilonproteobacteria, pp. 922–1143.
- López, L.R., Bezerra, T., Mora, M., Lafuente, J., Gabriel, D., 2016. Influence of trickling liquid velocity and flow pattern in the improvement of oxygen transport in aerobic biotrickling filters for biogas desulfurization. *J. Chem. Technol. Biotechnol.* 4, 1031–1039.
- Lu, H., Chandran, K., Stensel, D., 2014. Microbial ecology of denitrification in biological wastewater treatment. *Water Res.* 64, 237–254.
- Montebello, A.M., Bezerra, T., Rovira, R., Rago, L., Lafuente, J., Gamisans, X.,

- Campoy, S., Baeza, M., Gabriel, D., 2013. Operational aspects, pH transition and microbial shifts of a H<sub>2</sub>S desulfurizing biotrickling filter with random packing material. *Chemosphere* 93, 2675–2682.
- Montebello, A.M., Mora, M., López, L.R., Bezerra, T., Gamisans, X., Lafuente, J., Baeza, M., Gabriel, D., 2014. Aerobic desulfurization of biogas by acidic biotrickling filtration in a randomly packed reactor. *J. Hazard. Mater.* 280, 200–208.
- Mora, M., Fernandez, M., Gomez, J.M., Cantero, D., Lafuente, J., Gamisans, X., Gabriel, D., 2015. Kinetic and stoichiometric characterization of anoxic sulfide oxidation by SO-NR mixed cultures from anoxic biotrickling filters. *Appl. Microbiol. Biotechnol.* 99, 77–87.
- Muñoz, R., Meier, L., Diaz, I., Jeison, D., 2015. A review on the state-of-the-art of physical/chemical and biological technologies for biogas upgrading. *Rev. Environ. Sci. Biotechnol.* 14, 727–759.
- Narasimharao, P., Häggblom, M.M., 2006. *Sedimenticola selenatireducens*, gen. nov., sp. nov., an anaerobic selenate-respiring bacterium isolated from estuarine sediment. *Syst. Appl. Microbiol.* 29, 382–388.
- Portune, K.J., Pérez, M.C., Álvarez-Hornos, F.J., Gabaldon, C., 2014. Investigating bacterial populations in styrene-degrading biofilters by 16S rDNA tag pyrosequencing. *Appl. Microbiol. Biotechnol.* 99, 3–18.
- Russ, L., Speth, D.R., Jetten, M.S.M., Op den Camp, H.J.M., Kartal, B., 2014. Interactions between anaerobic ammonium and sulfur-oxidizing bacteria in a laboratory scale model system. *Environ. Microbiol.* 16, 3487–3498.
- Soreanu, G., Béland, M., Falletta, P., Edmonson, K., Seto, P., 2008. Laboratory pilot scale study for H<sub>2</sub>S removal from biogas in an anoxic biotrickling filter. *Water Sci. Technol.* 57, 201–207.
- Yang, C., Chen, H., Zeng, G., Yu, G., Luo, S., 2010. Biomass accumulation and control strategies in gas biofiltration. *Biotechnol. Adv.* 28, 531–540.